Title: **Modeling Human Endometrial Decidualization from the Interaction between Proteome and Secretome**

Tamara Garrido-Gomez, Francisco Dominguez, Juan Antonio Lopez, Emilio Camafeita, Alicia Quiñonero, Jose Antonio Martinez-Conejero, Antonio Pellicer, Ana Conesa & Carlos Simón.

Institutions: Fundación IVI (FIVI)-Instituto Universitario IVI (IUIVI)-Universidad de Valencia, INCLIVA Valencia, Spain (T.G., A.Q., A.P., C.S.); Stem Cell Bank, Centro de Investigación Príncipe Felipe, Valencia, Spain (C.S.). Embryomics S.L (F.D.). Unidad de Proteómica, Centro Nacional de Investigaciones Cardiovasculares, CNIC, Madrid, Spain (JA.L., E.C.). iGenomix S.L. (J.MC.). Bioinformatics Department and Functional Genomics Node (INB), Centro de Investigación Príncipe Felipe, Valencia, Spain (A.C.).

Abreviated title: Proteomic and Secretomic of the Decidualization Process

Key terms: human endometrial stromal cells, decidualization, proteomic, secretome.

Word count : 3599 words

Correspondence and reprint requests should be addressed to: Carlos Simón. C/ Guadassuar, 1 Bajo. Valencia 46015. Phone: +34 963 45 55 60; Fax: +34 963 45 55 12. e-mail: csimon@ivi.es

Disclosure summary: The authors have nothing to disclosure.

Proteomic and secretomic have been used as hypothesis-free approaches together with complex bioinformatics to model the human decidual interactome for the first time.

ABSTRACT

Context: Decidualization of the human endometrium, which involves morphological and biochemical modifications of the endometrial stromal cells (ESCs), is a prerequisite for adequate trophoblast invasion and placenta formation.

Objective: This study aims to investigate the proteome and secretome of *in vitro* decidualized ESCs. These data were combined with published genomic information and integrated to model the human decidualization interactome.

Design: Prospective experimental case-control study.

Setting: A private research foundation.

Patients: Sixteen healthy volunteer ovum donors.

Intervention: Endometrial samples were obtained, and ESCs were isolated and decidualized *in vitro.*

Main Outcome Measures: Two-dimensional difference in-gel electrophoresis, matrix-assisted laser desorption/ionization-time-of-flight mass spectrometry, Western blot, Human Protein Cytokine Array, ELISA and bioinformatics analysis were performed.

Results: The proteomic analysis revealed 60 differentially expressed proteins (36 over- and 24 underexpressed) in decidualized versus control ESCs, including known decidualization markers (cathepsin B) and new biomarkers (transglutaminase 2, peroxiredoxin 4 and the ACTB protein). In the secretomic analysis, a total of 13 secreted proteins (11 up- and 2 down-regulated) were identified, including well recognized markers (IGFBP-1 and PRL) and novel ones (MPIF-1 and PECAM-1). This proteome/secretome profiles have been integrated into a decidualization interactome model.

Conclusions: Proteomic and secretomic have been used as hypothesis-free approaches together with complex bioinformatics to model the human decidual interactome for the first time. We confirm previous knowledge, describe new molecules and we have build-up a model for human *in vitro* decidualization as invaluable tool for the diagnosis, therapy and interpretation of biological phenomena.

INTRODUCTION

Decidualization of human endometrial stromal cells (ESCs) is essential for coordinated trophoblast invasion and placenta formation since its defect predisposes to related pregnancy complications, including miscarriage, preeclampsia, fetal growth restriction and preterm labor.

Unlike rodents, the decidual reaction in humans is a conceptus-independent process. It comprises morphogenic, biochemical and vascular modifications initiated by the presence of progesterone (P) after proper estrogen (E2) priming (1). Morphologically, it is characterized by elongated fibroblast-like ESCs transformed into enlarged round cells with specific ultrastructural modifications, accompanied by the secretion of specific markers such as prolactin (PRL) and the insulin-like growth factor binding protein-1 (IGFBP-1) (2), plus extracellular matrices such as laminin, type IV collagen, fibronectin and heparin sulphate proteoglycan as part of their differentiation program (3, 4, 5). The onset of this process in the ESCs surrounding the terminal spiral arteries marks the end of the window of receptivity, where embryo adhesion to the endometrial epithelium can occur.

The majority of our knowledge of the regulation and mechanisms of human decidualization has been generated from *in vitro* model systems. The exposure of primary ESC cultures to P for 7-9 days, alone or in combination with E2, triggers the expression of decidual markers (6, 7, 8). This response is mediated by a gradual increase in intracellular cAMP levels and is abrogated in the presence of PKA inhibitors. The addition of dibutyryl cAMP (dbcAMP) leads to the *in vitro* decidualization of ESCs, which is used as a non hormonal decidualization stimulus (9, 10).

Microarray studies of decidualized ESCs have demonstrated a striking deregulation of genes associated with the extracellular matrix and tissue integrity, which suggests that these changes are prominent features (11, 12). Gene expression is only one dimension of the complex regulatory network that allows cells to respond to intracellular and extracellular signals. An initial attempt to use proteomic technologies to understand *in vitro* decidualization was published by Han et al. (13), and was based on surface-enhanced laser desertion/ionization time-of-flight mass spectrometry (SELDI-TOF-MS). Six

peaks detected by H4 and CM10 ProteinChips were found with a different expression between the non-decidual and 8-Br-cAMP-induced decidual cells corresponding to potential protein candidates (13).

Nevertheless, a comprehensively wide proteomic analysis underlying the mechanisms involved in the decidualization process is lacking. In the present study, we performed an in-depth analysis of the intracellular and secreted proteins during *in vitro* ESCs decidualization using a proteomic approach by combining gel-based methods and protein arrays. The information obtained has been integrated with the available genomic data (14) using state-of-the-art bioinformatic methods, resulting in the modeling of the human stromal decidualization process *in vitro*.

SUBJECTS AND METHODS

Subjects

This project received institutional review board approval by the Ethics Committee of IU-IVI (Valencia, Spain). Endometrial samples were acquired for research after obtaining a written consent from patients. A total of 16 human endometrial biopsies were collected on the day of oocyte retrieval from healthy ovum donors aged between 18 and 32. They were obtained with a pipelle catheter (Genetics, Belgium) under sterile conditions, processed and the stromal compartment was separated.

In vitro decidualization was induced by culturing ESCs in media containing progesterone and 17β-estradiol for 12 days. Decidualization was confirmed morphologically and by IGFBP-1 and PRL levels. For the proteomic study, 11 sets of samples (control vs. decidualized cells) were analyzed by fluorescence difference in-gel electrophoresis (2D-DIGE) and matrix-assisted laser desorption/ionization-mass spectrometry (MALDI-MS) technology. The **partial** secretomic analysis was performed with 7 of these 11 sets of samples using a human protein cytokine array. **The number of samples analyzed by secretomic was based on the balance between proper n number that assure credibility and financial constrains.** Validations of the results were performed by Western blot and ELISA with 4 sets of samples used in DIGE and the protein arrays analysis, and with the 5 sets outside the sample cohort. An extensive bioinformatics analysis was performed to integrate the proteome and secretome profiles together with the genomic information present in public databases.

Isolation, culture and decidualization of ESCs

Endometrial biopsies were subjected to mild collagenase digestion as previously described (6). ESCs were isolated and grown in 24-well plates using a DMEM/F12 medium containing 10% charcoal-stripped fetal bovine serum (FBS) and 0.1% antibiotics. After confluence, the medium was replaced with fresh media containing 2% FBS and supplemented with 5 ug/mL ascorbic acid and 10 ug/mL transferrin. Decidualization *in vitro* was induced by adding progesterone (1 μmol/L) and 17β-estradiol (30 nmol/L) for 12 days. The growth medium with hormones was renewed every 3 days. Control ESCs were cultured

in parallel over 12 days without hormonal treatment. The conditioned media from four wells were collected and pooled every 3 days, and cells were collected on day 9 of culture. The conditioned media was analyzed by ELISA for IGFBP-1 (Raybiotech) and PRL (Abbott Axsym System) levels.

Proteomic analysis

Proteins were extracted from decidual and control cells directly in lysis buffer (7 M urea, 2M thiourea, 4% CHAPS and 30 mM Tris-pH 8.5) containing 50 mM DTT and complete protease inhibitors tablets (Boehringuer) using the 2D Grinding Kit (GE Healthcare, Chalfont St Giles, UK). The suspension was shaken for 40 min at room temperature and centrifuged at 16000g for 15 min. Interfering components were removed using the 2D Clean Up Kit (GE Healthcare), and proteins were resuspended in lysis buffer. The protein concentration was determined using the RD/DC Protein Assay (Bio-Rad Laboratories, Hercules, CA, USA).

Proteins were labeled according to the manufacturer's indications (GE Healthcare). Briefly, 50 µg of decidual and control protein extracts were minimally labeled with 400 pmol of the Cy3 or Cy5 fluorescent cyanine dyes on ice in the dark for 30 min. To avoid any possible bias by labeling efficiency, we labeled half the samples from each group with Cy3 dye and the other half with the Cy5 dye. An internal standard, containing equal amounts of each cell lysate, was labeled with the fluorescent Cy2 dye and used for all the experiments. The labeling reaction was quenched with 1 µl of 10 mM lysine on ice for 10 min in the dark. The decidual and control protein extracts, and the internal standard protein samples, were combined and run in a single gel (150 µg total proteins). Protein extracts were applied by rehydration in immobilized pH gradient (IPG) strips (24 cm, pH 3-11, nonlinear) and subjected to isoelectrofocusing in an IPGphor Isoelectric Focusing System II (GE Healthcare) according to the manufacturer´s recommendations. After the first dimension, strips were equilibrated in SDS equilibration buffer (75 mM Tris pH 8.8, 6 M urea, 30% (v/v) glycerol, 2% (w/v) sodium dodecyl sulfate (SDS), traces of bromophenol blue) containing 1% (w/v) DTT for 15 min, and thereafter in SDS equilibration buffer containing 4% (w/v) iodoacetamide for another 15 min. Then proteins were separated on 10-12.5% SDS-PAGE gels using an Ettan Dalt Six device (GE Healthcare) at 25ºC until the tracking dye had migrated off the bottom of the gel.

Fluorescence images of the gels were acquired on a Typhoon 9400 scanner (GE Healthcare) and relative protein quantification was performed using the DeCyder software, v 7.0 (GE Healthcare), as previously described (15).

These spots were manually excised from the silver-stained gels and digested with trypsin in accordance with the protocol of Shevchenko et al. (16), save minor modifications. Briefly, MALDI samples were prepared and automatically analyzed in an Ultraflex MALDI-TOF/TOF mass spectrometer (Bruker Daltonik) (17) with an automated analysis loop using internal mass calibration, controlled by the flexControl 2.2 software (Bruker Daltonik). MALDI-MS spectra were acquired by averaging 300 individual spectra in the positive ion reflector mode at 50 Hz laser frequency in a mass range from 800 to 4000 Da. An internal calibration of the MALDI-MS mass spectra was performed using two trypsin autolysis ions with m/z ¼ 842.510 and m/z ¼ 2211.105. The precursor ions with a signal-to-noise ratio of ≥20 in the MALDI-MS mass spectrum were submitted to a fragment ion analysis in the tandem (MS/MS) mode. The MALDI-MS and MS/MS data were combined through the BioTools 3.0 program (Bruker Daltonik) to search a nonredundant protein database (NCBInr; ~6.5 x 10^6 entries, National Center for Biotechnology Information, Bethesda US) using the Mascot 2.2.1 software (Matrix Science, London, UK) (18). Protein scores over 80 were considered significant ($P < 0.05$).

Western blot

Proteins (80 µg) from the decidual and control cells were separated by discontinuous electrophoresis (stacking gel 4% polyacrylamide and resolving gel 12% polyacrylamide) for 1 h at 180 V. Later, proteins were transferred onto the polyvinylidene fluoride (PVDF) membrane by wet electroblotting using the tris/glycine transfer buffer (Biorad) for 4 h at 4ºC with shaking. PVDF membranes were blocked in PBS and 5% dry non-fat milk at room temperature for 1 h. Immunoblotting was performed with primary antibodies; 2.5 µg /ml mouse monoclonal transgelin, 2 µg/ml mouse monoclonal alpha actinin, 2 µg /ml mouse monoclonal transglutaminase 2 and 0.25 µg/ml mouse monoclonal cathepsin B (all of Abcam, Cambridge, UK) at 4ºC. Then membranes were incubated with the 1:2000 dilution of the polyclonal goat anti-rabbit IgG-HRP (DakoCytomation, CA) and the polyclonal rabbit anti-goat IgG-HRP (DakoCytomation, CA) at room temperature for 1 h. PVDF

membranes were analyzed with the ECL Western Blotting Analysis System (GE Healthcare, Freiburg, Germany) and were photographed using Fujifilm LAS-300. The subsequent densitometry analysis of bands was done with the Fujifilm Multi Gauge V3.0 program. Membranes were stripped and incubated with a monoclonal mouse antihuman 0.4 mg/ml GAPDH antibody (Abcam, Cambridge, UK) and processed as above.

Secretomic analysis

The conditioned media obtained from 7 sets of decidual and control cells collected on day 9 were compared using the Human Cytokine Antibody Array G Series 2000 (Raybiotech). Arrays contained 174 human cytokines which could be simultaneously compared in a single experiment between two given conditions (19, 20). Antibody array slides were blocked for 30 min at room temperature prior to media incubation. Briefly, the decidual and control conditioned media (100 µL each) and the media without cells (DMEN/F12 with 2% SBF) (100 µL) were incubated in three different membranes (arrays VI, VII and VIII) for 2 h at room temperature. After sample incubation and washing, a diluted biotin-conjugated anti-cytokine primary antibody was applied to each membrane for 2 h at room temperature. After washing, diluted fluorescent dye-conjugated streptavidin was added to the membranes for 2 h at room temperature in the dark. Slides were washed and water droplets were removed by centrifuging at 1000 rpm for 3 min. Then slides were left to dry completely in air for at least 20 min. Arrays were scanned in an Axon 4100A scanner (Molecular Devices, Sunnyvale, CA, USA) and data were extracted with the GenePix Pro 6.0 software (Molecular Devices).

The GenePix Pro 6.0 software was used for the array image analysis and to calculate spot intensity measurements which were considered raw data. Spot intensities (medians) with background subtraction were transformed to the log2 scale. Before quantile normalization, data were represented in a box plot to know the data distribution and subtract abnormal microarray data. Replicates per protein symbol were merged.

The R-statistical software system was used as a tool for these purposes and the downstream analysis. The protein expression profile was determined by comparing decidual and control conditioned media with parametric and nonparametric tests, and two criteria were used to define those proteins with

altered abundance among the different sample sets: an absolute fold change of 1.5 or more, and a corresponding p-value lower than 0.05.

ELISA analysis

The conditioned media from both decidual and control cells were evaluated in duplicate using the commercial ELISA kit for MPIF-1, IL-6 and MCP-3 (Raybiotech) and IL1R-II (Hycult biotech). Sample values (pg/mL) were determined using the standard curve.

Statistical analysis

ELISA analysis data and levels of prolactin and IGFBP-1 secretions were processed for statistical evaluation. Quantitative data are presented as mean ± SD. A nonparametric Mann-Whitney U-test was done to compare the average ratios for each molecule (ng/mL) between decidual and control samples. Statistical significance was defined as a P-value of <0.05.

Bioinformatics analysis of the results

A bioinformatics analysis pipeline was developed to integrate the proteome and secretome profiles together with the information present in public databases and data repositories.

An interaction network between those proteins, detected as being differentially regulated both intra- and extracellularly, was created using the Snow application (http://snow.bioinfo.cipf.es) (21) present in the functional analysis suite, Babelomics (http://www.babelomics.org) (22). Although the progesterone and estradiol receptors (PGR, ESR1 and ESR2) were not detected as being differentially expressed, they were also included in the set of interacting proteins as they represent the primary entrance for the hormonal signals that trigger decidualization. To construct the interaction network, the curated human interaction database available at Snow was used, which includes the physical protein-protein interactions detected by at least two different experimental methods, and the incorporation of one connecting protein (not present in the experimental data) was allowed. This decidualization interactome **defined as the network of proteins identified from the interaction between proteome and secretome,** was further completed by including the information available on the transcription factors

(TFs) regulating the expression of the coding genes for all the proteins in the network. Transcription factor data were obtained from the Jaspar database (23), which is included in Babelomics. Additionally, the gene expression information of the decidualization process (14) was collected and crossed with the proteomic data to identify the gene whose differential expression was observed at both the gene expression and protein levels. All the proteins in the resulting network were manually reviewed and classified into 19 different functional categories that best described the diversity of the functions in our dataset. Finally, the network was visualized using the Cytoscape software (24).

RESULTS and DISCUSSION

After 9 days of culture, *bona fide in vitro* decidualized ESCs were identified by the appearance of a rounded decidual phenotype (Fig. 1A&1B) with a significant increase of IGFBP-1 (98.38±48.07ng/ml) and PRL (60.27±23.71ng/ml) (Fig. 1C&1D). Only those decidualized vs. control ESCs pairs (n=16) with a significant increase ($P<0.005$) in PRL and IGFBP-1 were used for further analyses.

Proteomic analysis of decidualized ESC and validation by Western blot

Over 2,500 spots were detected across the pI range (3-11 NL) with the DIA module (DeCyder^{TM}). The differentially expressed proteins were excised and identified by MALDI peptide mass fingerprinting and/or peptide fragmentation using the Mascot search engine (Fig. 2A). A list of 60 proteins was identified with significantly different abundance between decidualized and controls ESCs: 36 up- and 24 were down-regulated (Table 1). Among the identified spots, proteins related with the cytoskeleton (alpha-actinin, gelsolin and keratin 7), redox homeostasis (superoxide dismutase and peroxiredoxin 4), metabolism (triosephosphate isomerase 1 and monoglyceride lipase), and protein folding/degradation (cathepsin B and protein disulfide isomerase) were found. In some cases, the same protein was identified in two different spots (e.g., caldesmon spots 13 and 14), suggesting the occurrence of posttranslational modifications. In addition, two different co-migrating proteins were identified in one spot (e.g., spot 2, proteins disulfide-isomerase and ribonuclease inhibitor).

For validation purposes, transgelin and actinin alpha 1, as significantly underexpressed and cathepsin B and transglutaminase 2 as significantly overexpressed, were analyzed by Western blot in 4 sets of the decidualized vs. control ESCs used in the DIGE analysis. The results obtained demonstrate a similar regulation which was reported in the proteomic analysis. Cathepsin B and transglutaminase were up-regulated (fold change 1.4 and 1.7, respectively). In contrast, alpha actinin and transgelin significantly reduced in the decidualized vs. control cells (fold change -4.5 and -6.1, respectively) (Fig. 2B). Four additional sets of decidualized and control cells (n=4) outside the initial DIGE cohort were analyzed to extend the results to the general population. The results matched those previously reported (Fig. 2C).

Secretomic analysis of decidualized ESCs and validation by ELISA

The decidual and control-conditioned media (n=7) collected on day 9 of culture were comparatively analyzed using a protein array (Supplementary Fig. 1). Table 2 presents the differentially secreted proteins; the fold-change and the raw p-values are also shown. As expected, proteins such as IGFBP-1 and prolactin significantly increased (raw $p < 0.05$) in the decidual media. It is noteworthy that novel secreted decidualization markers such as MPIF-1, IL-10 beta receptor, IL-21 receptor, PECAM-1, the decoy receptor IL-1R II, CD80, leptin receptor also increased (> 2-fold change, raw $p < 0.05$). Only two proteins, IL-6 and MCP-3, significantly reduced in the decidual versus the control media (raw $p < 0.05$).

ELISA validation was performed for two overexpressed (PECAM, MPIF-1) and two underexpressed (IL-6 and MCP-3) secreted proteins. ELISA experiment was performed in 4 sets of decidualized vs. control-conditioned media collected on day 9, which had already been used in the secretome study, thus demonstrating a similar regulation to the array experiment (Fig. 3A). As expected, MPIF-1 and ILR1-RI were significantly up-regulated and MCP-3 and IL-6 significantly reduced in the decidualized compared to the ESC control media. We also analyzed the 5 additional ESC decidualized vs. control-conditioned media obtained outside the array cohort, thus corroborating the results reported by the array (Fig. 3B). The results were evaluated with a Mann-Whitney U-test and demonstrate statistically significant differences.

Modeling the decidualization interactome

A total of 47 and 18 unique intracellular and extracellular proteins, respectively, were identified as being differentially expressed by our proteomic analysis. Of these 65 proteins, 44 were joined by the Snow software into a highly interconnected network where one additional protein between each protein pair was allowed. This network contained a total of 132 proteins (44 native and 88 added by the Snow software) and 378 interactions (Fig. 4) (Supplementary Table I). A total of 33 transcriptor factors (TFs) were found to regulate the expression of the 65 proteins and were also included in the net. Interestingly,

5 of these TFs (GATA2, GATA3, SOX10, SPIB, TFAP2A) were classified as “specifiers” by the Fantom database (25), which implies that these TFs are expressed in a tissue-specific fashion, where 6 TFs (USF1, ARID3A, ETS1, BRCA1, NFIC, YY1) were “facilitators”, or broadly expressed regulators. By crossing the proteomic data with the set of 734 differentially expressed genes **with our proteomic data, were identified 15 genes differentially expressed at both mRNA expression and protein level.** These genes include native proteins (Caldesmon 1, actinin alpha 4, transgelin, calponin), transcription factors (NR4A, BRCA1) and additional nodes (IGFBP1, laminin A/C, vimentin, vinculin, cyclin-dependent kinase 1, serpin peptidase inhibitor E).

Functional annotation of the identified decidualization components reveals a number of interesting aspects in the biology of this process. First, a large proportion of the intracellular regulated proteins related to cytoskeleton organization, extracellular matrix composition and the connection between the two cellular architectural complexes. Initiation of decidualization was accompanied by a significant up-regulation of actin (beta and gamma actins), while a disruption of the actin filaments altered the decidualization course (26). It has been recently demonstrated that destabilization of the cytoskeleton accelerates decidualization, whereas increased phosphorylation of the myosin light chain prevents decidualization (27). Given the importance of cytoskeletal restructuring during decidualization, it is not altogether surprising that 28% of the proteins found actually relate to the cytoskeleton and are regulated during decidualization. Transgelin, also known as smooth muscle protein 22 (SM22) (28), has not been described before in human decidualization and is, therefore, a novel intracellular biomarker.

Second, substantial modifications in the extracellular matrix were reflected by a down-regulation of metalloproteases (MMP2, MMP3 and MMP14), with an increase in protease inhibitors such as TIMP1. Their balance is fundamental for the controlled invasion of trophoblast by decidual cells.

Steroid hormones (E and P) play a pivotal role and their receptors PGR, ESR1 and ESR2 have been incorporated into the decidualization interactome to analyze relations with significant proteins. The appropriate functioning of steroid hormone receptors depends on their interaction with molecular chaperones such as chaperonin containing TCP1, protein disulfide isomerise, and heat shock protein 27 which, interestingly, up-regulated in decidualized ESCs.

Decidual cells are a source of growth factors and cytokines that support/control trophoblast invasion (29, 30). A total of 13 differentially secreted proteins were found (11 up- and 2 down-regulated). Among the most regulated well recognized markers, IGFBP-1 (6.51-fold increase) and PRL (2.44-fold increase) were present, along with a novel one, MPIF-1 (7.02-fold increase). This molecule also known as CCL23, shows chemotactic activity for monocytes, resting T-lymphocytes and neutrophils, but not for activated lymphocytes. This chemokine participates in cell-cell signaling, chemotaxis, immune and inflammatory responses (31). Human MPIF-1 induces endothelial cell migration and tube formation in a three-dimensional matrigel (3D) via CCR1 receptor binding (32). Neutralization with the anti-MPIF1 and anti-CCR1 antibodies resulted in a blockage of the MPIF1-activated invasion of HUVECs. These results indicate that MPIF-1 may play a direct role in angiogenesis.

IL-6 and MCP-3 were significantly down-regulated compared to the non decidualized hESCs. Exogenous IL-6 has a stimulatory effect on first trimester cytotrophoblast invasion, and anti-IL-6 inhibited this effect (33). MCP-3, also known as CCL7, is a chemotactic factor that binds to different receptors CCR1, CCR2 and CCR3. Migration assays have employed the trophoblast cell line that most closely resembles the extravillous cytotrophoblast (AC1M-88), showing that trophoblast migration does not occur in response to CCL7 (34).

In conclusion, proteomic and secretomic approaches integrated with genetic background, have been employed in this work using complex bioinformatics to model the human decidual interactome for the first time. The results reveal that the implicated proteins are included in different categories, mainly relating to *actin cytoskeleton regulation, cell adhesion, protein folding and degradation, redox homeostasis and signal transduction.* We present this model as a tool for the diagnosis, therapy and interpretation of biological phenomena **in health and disease models such as preeclampsia or miscarriages of endometrial origin where the alteration of the decidua may play a prevalent role.**

BIBLIOGRAPHY

1. **Ramathal CY, Bagchi IC, Taylor RN, Bagchi MK** 2010 Endometrial decidualization of mice and men. Semen Reprod Med 28:17-26.

2. **Irwin JC, De las Fuentes L, Dsupin BA, Guidice LC** 1993 Insulin-like growth factor regulation of human stromal cell function: coordinate effects on insulin-like growth factor binding protein-1, cell proliferation and prolactin secretion. Regul Pept 48:165-177

3. **Dunn CL, Kelly RW, Critchley HO** 2003 Decidualization of the human endometrial stromal cell: an enigmatic transformation. Reprod Biomed 7:151-161

4. **Tabanelli S, Tang B, Gurpide E** 1992 In vitro decidualization of human endometrial stromal cells. J Steroid Biochem Mol Biol 42:337-44

5. **Irwin JC, Utian WH, Eckert RL** 1991 Sex steroids and growth factors differentially regulate the growth and differentiation of cultured human endometrial stromal cells. Endocrinology 129:2385-2392.

6. **Simón C, Piquette GN, Frances A, Danasouri I, Irwin JC, Polan ML** 1994 The effect of interleukin-1 beta on the regulation of IL-1 receptor type I messenger ribonucleic acid and protein levels in cultured human endometrial stromal and glandular cells. J Clin Endocrinol Metab 78:675-82

7. **Irwin JC, Kirk D, King RJ, Quigley MM, Gwatkin RB** 1989 Hormonal regulation of human endometrial stromal cells in culture: an in vitro model for decidualization. Fertil Steril 52:761-768

8. **Gellersen B, Brosens J** 2003 Cyclic AMP and progesterone receptor cross-talk in human endometrium: a decidualizing affair. J Endocrinol 178:357-372

9. **Tang B, Guller S, Gurpide E** 1993 Cyclic adenosine′,3′ -monophosphate induces prolactin expression in stromal cells isolated from human proliferative endometrium. Endocrinology 133:2197–2203.

10. **Brar AK, Frank GR, Kessler CA, Cedars MI, Handwerger S** 1997 Progesterone-dependent decidualization of the human endometrium is mediated by cAMP. Endocrine 6:301-307.

11. **Popovici RM, Lee-Chuan K, Giudice L** 2000 Discovery of new inducible genes in vitro decidualized human endometrial stromal cells using microarray technology. Endocrinology 143:3510-3514

12. **Brar AK, Handwerger S, Kessler CA, Aronow BJ** 2001 Gene induction and categorical reprogramming during *in vitro* human endometrial fibroblast decidualization. Physiol Genomics 7:135–148

13. **Oh KJ, Choi HJ, Yoon MS, Hwang JH, Chang S, Kim YS, Han JS** 2008 Rapid analysis of proteomic biomarkers expressed in human endometrial stromal cells during decidualization. Arch Pharm Res 10:1247-1255.

14. **Aghajanova L, Horcajadas JA, Weeks JL, Esteban FJ, Nezhat CN, Conti M, Giudice LC** 2010 The protein kinase A pathway-regulated transcriptome of endometrial stromal fibroblasts reveals compromised differentiation and persistent proliferative potential in endometriosis. Endocrinology 151:1341-55.

15. **Dominguez F, Garrido-Gómez T, López JA, Camafeita E, Quiñonero A, Pellicer A, Simón C** 2009 Proteomic analysis of the human receptive versus non-receptive endometrium using differential in-gel electrophoresis and MALDI-MS unveils stathmin I and annexin A2 as differentially regulated. Hum Reprod 24:2607-2617.

16. **Shevchenko A, Tomas H, Vorm O, Havlis J, Mann M** 2006 In-gel digestion for mass spectrometric characterization of proteins and proteomes. Nat Protoc 1:2856-2860.

17. **Suckau D, Resemann A, Schuerenberg M, Hufnagel P, Franzen J, Holle A** 2003 A Novel MALDI LIFT-TOF/TOF mass spectrometer for proteomic. Anal Bioanal Chem 376:952-965.

18. **Perkins DN, Pappin Dj, Creasy DM, Cottrell JS** 1999 Probability-based protein identification by searching sequence databases using mass spectrometry data. Electrophoresis 20:3551-3567.

19. **Dominguez F, Gadea B, Esteban FJ, Horcajadas JA, Pellicer A, Simón C** 2008 Comparative protein-profile analysis of implanted versus non-implanted human blastocysts. Hum Reprod 23:1993-2000.

20. **Dominguez F, Gadea B, Mercader A, Esteban FJ, Pellicer A, Simón C** 2010 Embryologic outcome and secretome profile of implanted blastocysts obtained after coculture in human endometrial epithelial cells versus the sequential system. Fertil Steril 93:774-782.

21. **Minguez P, Götz S, Montaner D, Al-Shahrour F, Dopazo J** 2009 SNOW, a web-based tool for the statistical analysis of protein-protein interaction networks. Nucleic Acids Res 1:109-114.

22. **Medina I, Carbonell J, Pulido L, Madeira SC, Goetz S, Conesa A, Tárraga J, Pascual-Montano A, Nogales-Cadenas R, Santoyo J, García F, Marbá M, Montaner D, Dopazo J** 2010 Babelomics: an integrative platform for the analysis of transcriptomics, proteomic and genomic data with advanced functional profiling. Nucleic Acids Res 38:210-213.

23. **Portales-Casamar E, Thongjuea S, Kwon AT, Arenillas D, Zhao X, Valen E, Yusuf D, Lenhard B, Wasserman WW, Sandelin A** 2010 JASPAR 2010: the greatly expanded open-access database of transcription factor binding profiles. Nucleic Acids Res 38:105-110.

24. **Shannon P, Markiel A, Ozier O, Baliga NS, Wang JT, Ramage D, Amin N, Schwikowski B, Ideker T** 2003 Cytoscape: a software environment for integrated models of biomolecular interaction networks. Genome Research 13:2498-504.

25. **Ravasi T, Suzuki H, Cannistraci CV, Katayama S, Bajic VB, Tan K, Akalin A, Schmeier S, Kanamori-Katayama M, Bertin N, Carnicini P, Daub CO, Forrest AR, Gough J, Grimmond S, Han JH, Hashimoto T, Hide W, Hofmann O, Kamburov A, Kaur M, Kawaji H, Kubosaki A, Lassmann T, van Nimwegen E, MacPherson CR, Ogawa C, Radovanovic A, Schwartz A, Teasdale RD, Tegnér J, Lenhard B, Teichmann SA, Arakawa T, Ninomiya N, Murakami K, Tagami M, Fukuda S, Imamura K, Kai C, Ishihara R, Kitazume Y, Kawai J, Hume AD, Ideker T, Hayashizaki Y** 2010 An atlas of combinatorial transcriptional regulation in mouse and man. Cell 140:744-752.

26. **Ihnatowch I, Livak M, Reed J, Lanerolle P, Strakova Z** 2009 Manipulating actin dynamics affects human in vitro decidualization. Biol Reprod 81:222-230.

27. **Ihnatowch I, Hu W, Martin JL, Fazleabas AT, Lanerolle P, Strakova Z** 2007 Increased phosphorylation of myosin light chain prevents in vitro decidualization. **Endocrinology** 148:3176-3184.

28. **Nair RR, Solway J, Boyd DD** 2006 Expression cloning identifies transgelin (SM22) as a novel repressor of 92 kDa type IV collagenase (MMP-9) expression. J Biol Chem 281:26424-26436.

29. **Finn CA** 1997 The implantation reaction. Biology of the Uterus 77: 246–308.

30. **Glasser SR, Mulholland J, Mani SK** 1991 Blastocystendometrial relationships: reciprocal interactions between uterine epithelial and stromal cells and blastocysts. Trophoblast Res 5:229–280

31. **Patel VP, Kreider BL, Li Y, Li H, Leung K, Salcedo T, nardelli B, Pippalla V, Gentz S, Thotakura R, Parmelee D, Gentz R, Garotta G** 1997 Molecular and functional characterization of two

novel human C-C chemokines as inhibitors of two distinct classes of myeloid progenitors. J Exp Med 185:1163-1172.

32. **Son KN, Hwang J, Kwon BS, Kim J** 2006 Human CC chemokine CCL23 enhances expression of matrix metalloproteinase-2 and invasion of vascular endothelial cells. Biochem Biophys Res Commun 340:498-504.

33. **Jovanovic M, Vicovac L** 2009 Interleukin-6 stimulates cell migration, invasion and integrin expression in HTR-8/SVneo cell line. Placenta 30:320-328.

34. **Hannan NJ, Jones RL, White CA, Salamonsen LA** 2006 The chemokines, CXCL1, CCL14, and CCL4, promote human trophoblast migration at the feto-maternal interface. Biol Reprod 74:896-904.

FIGURES AND TABLES

Figure 1. *In vitro* decidualization.

(A) Morphology of human ESCs cultured without hormonal treatment for 9 days. (B) Decidualized human ESCs cultured with progesterone and 17β-estradiol for 9 days. (C&D) Prolactin & IGFBP-1 secretions measured by ELISA presented as ng/mL (mean± SD) in control (white bar) and decidualized (black bar) cultures on days 0, 3, 6, 9 and 12 of culture. * p-value < 0.05 **p-value< 0.005.

Figure 2. 2D-DIGE of decidualized **(D)** vs. control **(C)** ESCs and validation.

Individual proteins of control cells, decidual cells and a pooled internal standard were labeled with CyDyes, Cy3, Cy5 and Cy2 respectively, and were mixed and separated on a 2D gel using 24 cm pH 3-11 NL (left to right) strips in the first dimension and 10% PAGE-SDS gels in the second dimension. Gels were scanned to obtain images of the overlay of the two dyes (Cy3, Cy5) (A.1, A.2). The same gels, after fluorescence imaging, were silver-stained and scanned (A.3, A.4). The 53 protein spots found to be significantly deregulated in the decidualizated vs. the control samples (P< 0.05) are encircled. The proteins identified by in-gel trypsin digestion and MALDI-TOF/TOF are summarized in Table I.

Validation of the DIGE experiments of alpha-actinin, transgelin, cathepsinB and transglutaminase by Western blot. (B) Protein extracts from endometrial samples used in the DIGE experiments; bands correspond to 107 kDa alpha actinin and 23 kDa transgelin. Both significantly reduced in the decidualized versus the control cells (densitometry values of -4.5 and -6.1, respectively); 38 kDa cathepsin B and 90 kDa transglutaminase proteins were found up-regulated (densitometry values of 1.4 and 1.7, respectively) (C) validation experiments were also performed in a new set of samples which had not been previously analyzed in the DIGE cohort. The results matched the previous ones. GAPDH was used as a control to normalize protein abundance in all the experiments performed. The densitometric results are provided as the normalized values between the indicated markers and GAPDH.

Figure 3. Secretome profile validation of MPIF-1, IL1 RII, MCP-3 and IL-6 measured by ELISA in the conditioned media from the decidual (D) and control (C) ESCs.

(A) MPIF, IL1 RII, MCP-3 and IL-6 were analyzed in 4 experiments using conditioned media which had been already investigated in the secretome analysis.

(B) To validate the biological significance outside the sample cohort, 6 additional sets of control and decidual samples were used.

The results in pg/ml are shown as mean ±SD of the control- (white bar) vs. the decidual- (black bar) conditioned media for each molecule.

* p-value < 0.05, ** p-value < 0.01

Figure 4. Decidualization Interactome including the proteins detected in our study as differentially regulated, both intra- and extracellularly together with the information present in public databases and data repositories.

(Triangle) The significantly overexpressed proteins in our proteomic analysis, (Squaring) The significantly underexpressed proteins in our proteomic analysis, (Circle) Transcription factors, (Rhombus) Connecting proteins added to construct the interaction network.

(Pink Line) Direct interactions among the deregulated proteins found in our proteomic analysis. (Blue Line) Indirect interactions among the deregulated proteins through connecting proteins. (White Line) Interactions among the proteins and transcription factors. (Red Line) Interactions among all the proteins and PGR, ESR1 and ESR2.

Proteins are classified into 15 different functional categories, indicated by different colours in the legend (cytoskeleton, redox, exocytosis/endocytosis, cell adhesion/collagen/ECM, protein folding, protein degradation, DNA/RNA metabolism, lipid metabolism, heat shock protein, glycolisis, mitochondria, extracellular, signal transduction, cell cycle, angiogenesis).

The remarked proteins correspond to the identified gene whose differential expression was observed at both the gene expression and protein levels.

Table 1. Proteins identified by MALDI-TOF/TOF showing significant changes between the decidual and the control ESCs on day 9 of culture.

[a] Spot number as shown in the 2-DE silver gel in Fig. 2 (spots 1-53). [b]Average volume ratio (decidual/control) as calculated by the DeCyder BVA analysis. [c]Student t-test P-value. [d]Protein accession code from the SwissProt database. [e]Mascot score, [f]Expected value, [g]Theoretical molecular weight (Da), [h]pI. [i]Number of matched peptides and [j]protein sequence coverage for the most probable candidate as provided by Mascot. **Bold represent proteins validated by western blot analysis.**

Table 2. List of the secreted proteins modified by the decidualization effect.

[a] Protein name as shown in the protein array. [b]Fold change (decidual/control). [c]Statistical test P-value. [d]Protein description.

FIGURE 1

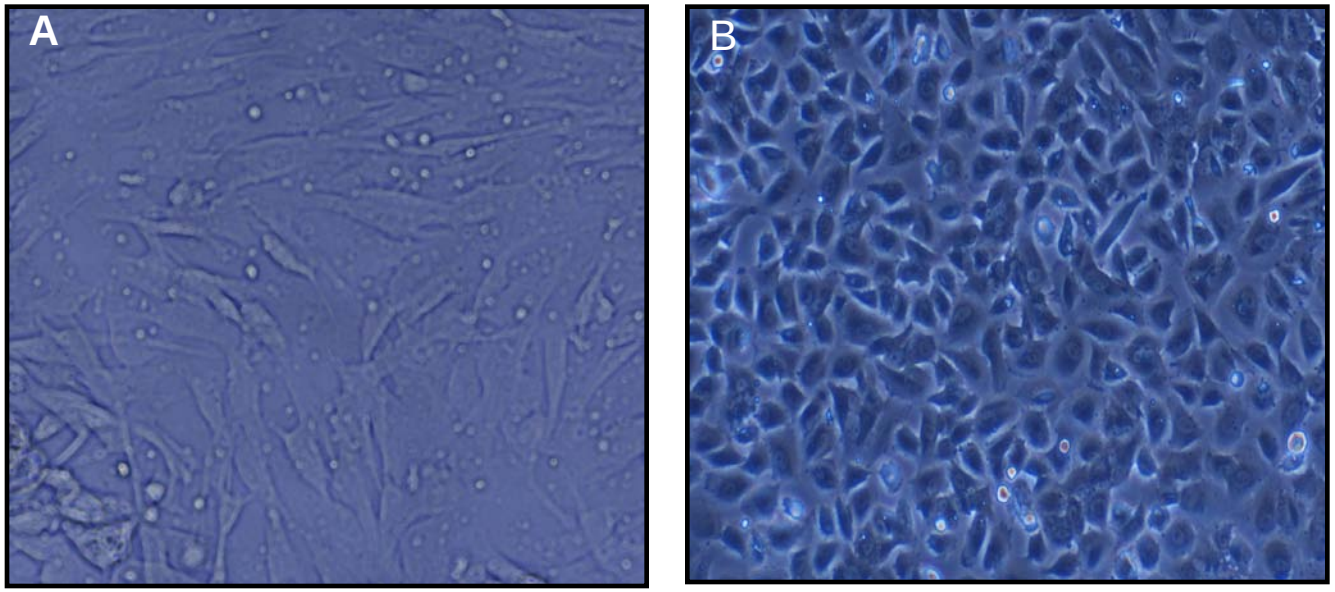
A
B

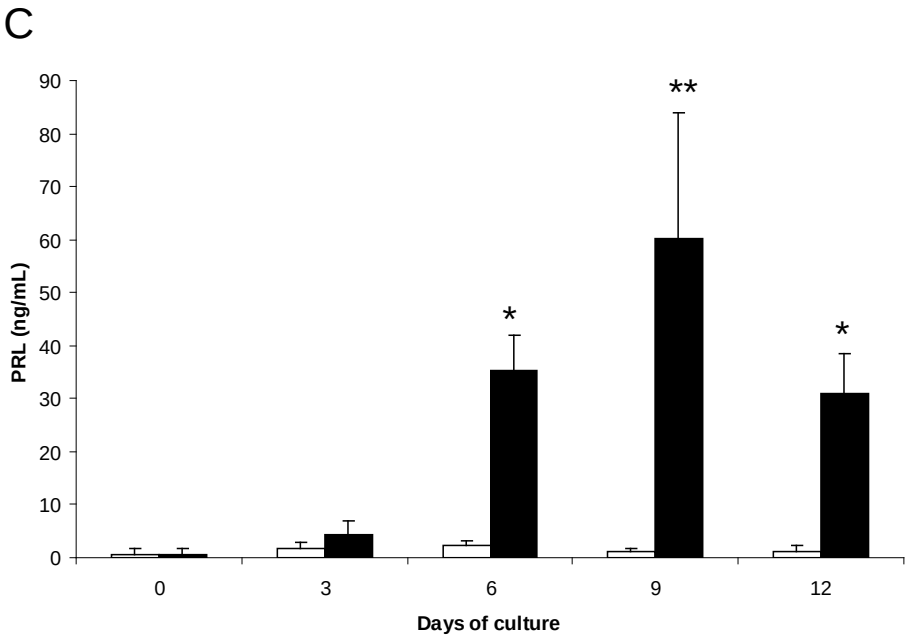
C
PRL (ng/mL)
90
80
70
60
50
40
30
20
10
0
0
3
6
9
12
Days of culture
*
**
*

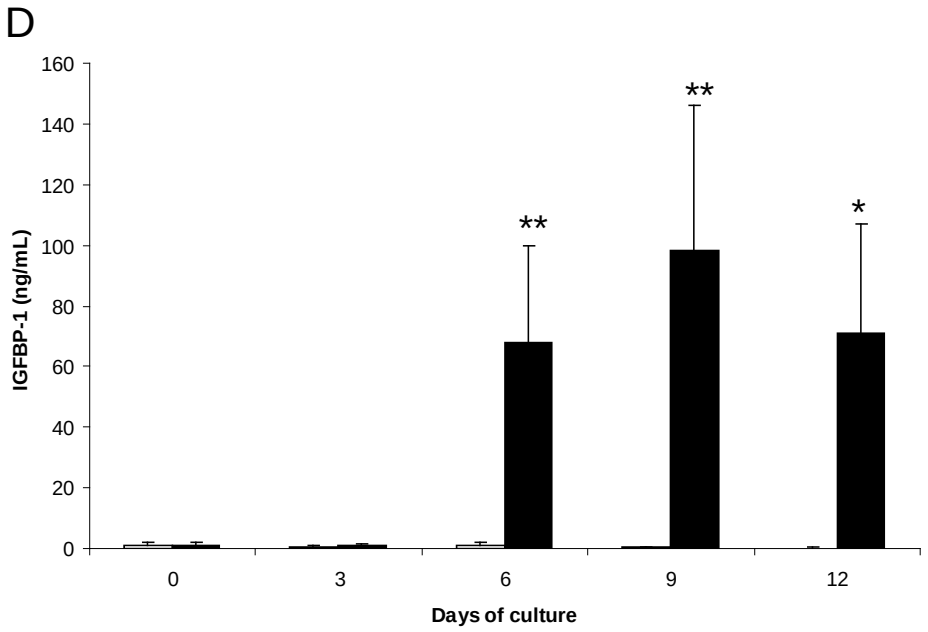
D
IGFBP-1 (ng/mL)
160
140
120
100
80
60
40
20
0
0
3
6
9
12
Days of culture
**
**
*

FIGURE 2

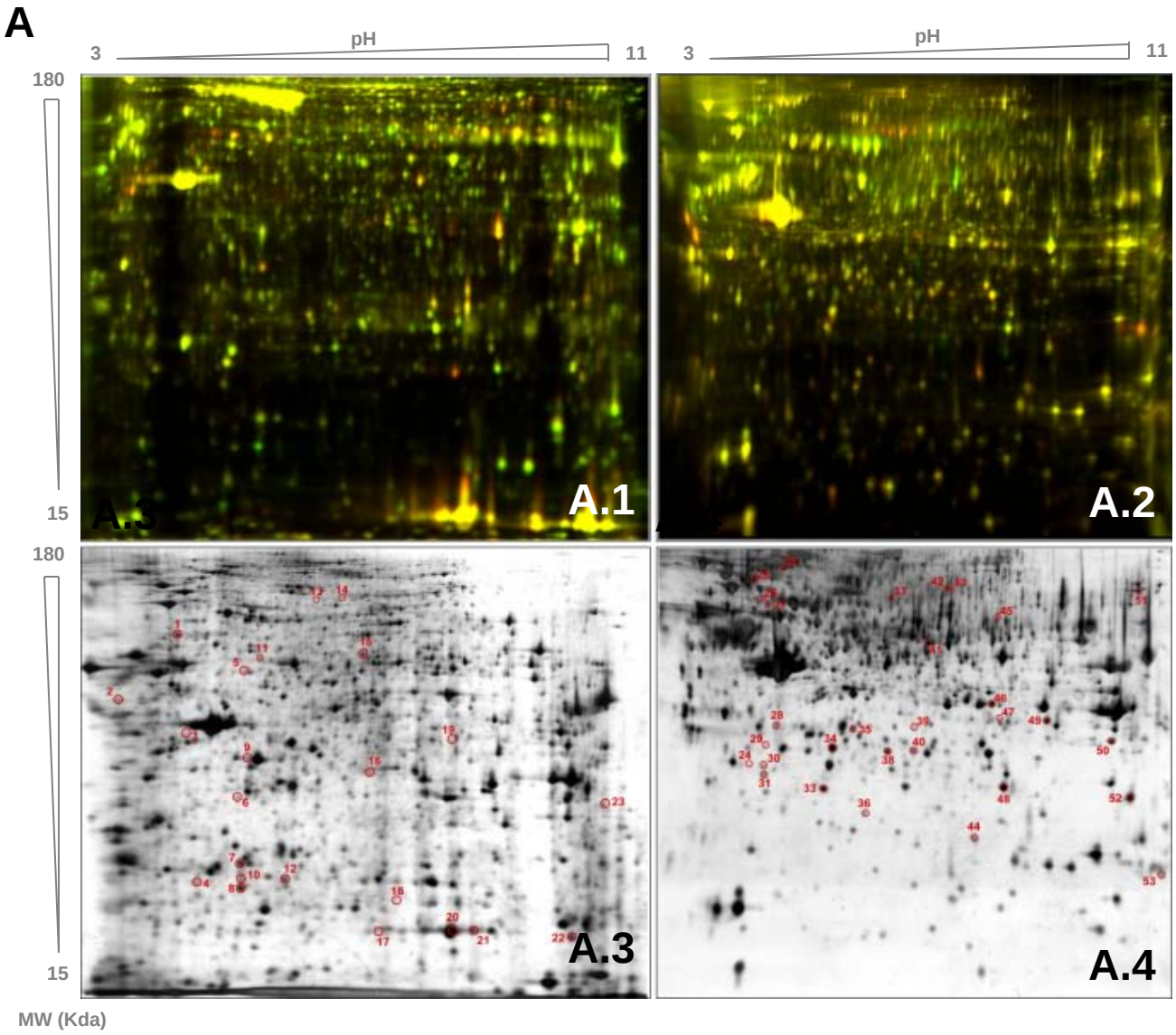
A
pH
3
11
180
15
A.1
A.2
A.3
A.4
MW (Kda)

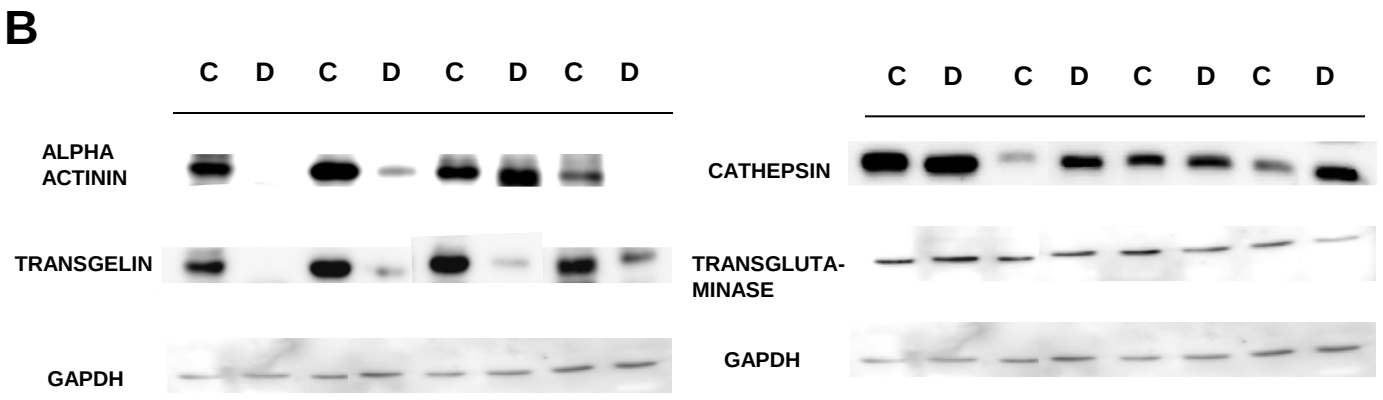
B
C D C D C D C D
ALPHA ACTININ
TRANSGELIN
GAPDH
C D C D C D C D
CATHEPSIN
TRANSGLUTA-MINASE
GAPDH

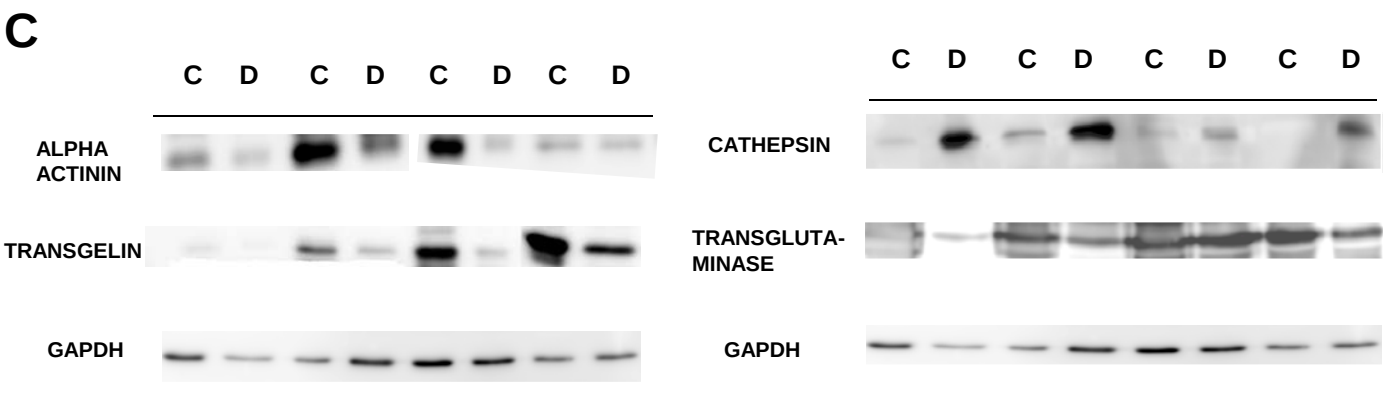
C
C D C D C D C D
ALPHA ACTININ
TRANSGELIN
GAPDH
C D C D C D C D
CATHEPSIN
TRANSGLUTA-MINASE
GAPDH

FIGURE 3

A

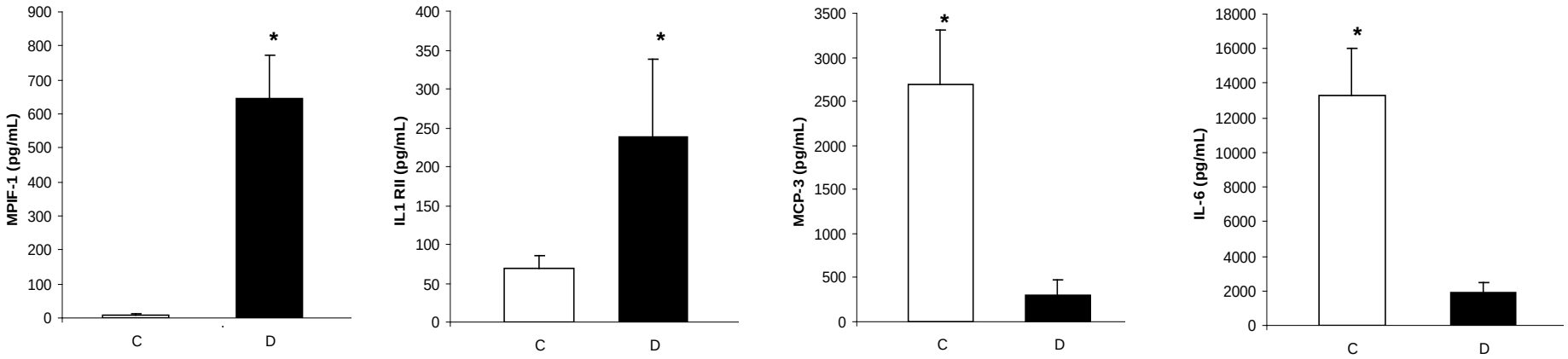
MPIF-1 (pg/mL)
900
800
700
600
500
400
300
200
100
0
*
C
D
IL1 RII (pg/mL)
400
350
300
250
200
150
100
50
0
*
C
D
MCP-3 (pg/mL)
3500
3000
2500
2000
1500
1000
500
0
*
C
D
IL-6 (pg/mL)
18000
16000
14000
12000
10000
8000
6000
4000
2000
0
*
C
D

B

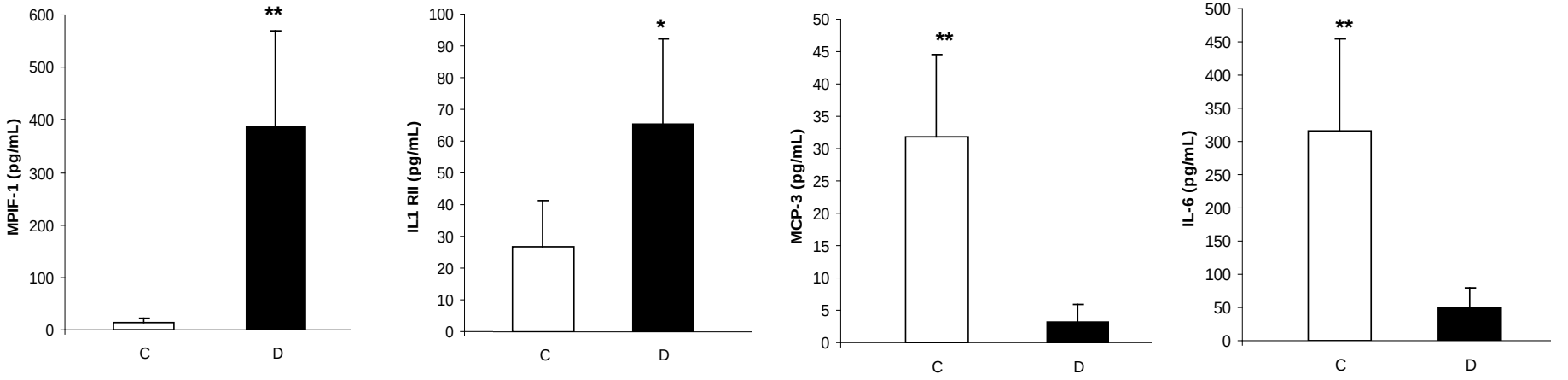
MPIF-1 (pg/mL)
600
500
400
300
200
100
0
**
C
D
IL1 RII (pg/mL)
100
90
80
70
60
50
40
30
20
10
0
*
C
D
MCP-3 (pg/mL)
50
45
40
35
30
25
20
15
10
5
0
**
C
D
IL-6 (pg/mL)
500
450
400
350
300
250
200
150
100
50
0
**
C
D

FIGURE 4

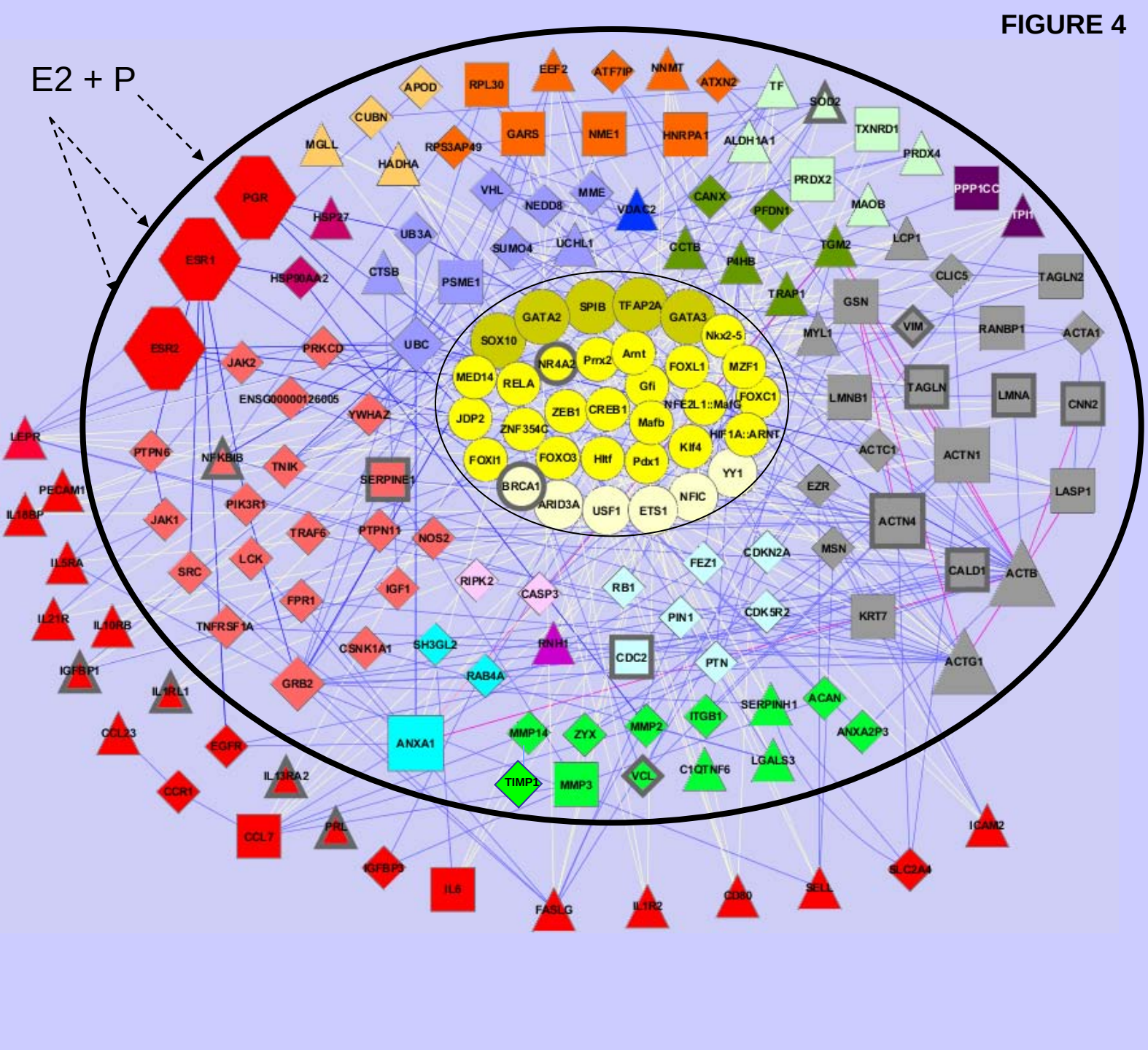

- Up-regulated proteins
- Down-regulated proteins
- TFs
- Connecting proteins
- Hormonal receptors
- Direct interaction
- Interaction connecting protein
- Protein-TF interaction

- DNA/RNA metabolism
- TF
- TF/facilitator
- TF/specifier
- angiogenesis
- apoptosis
- cell adhesion/collagen/ECM
- cell cycle
- cytoskeleton
- exocytosis/endocytosis
- extracellular
- glycolisis
- heat shock protein
- lipid metabolism
- mitochondria
- protein_degradation
- protein_folding
- redox
- signal transduction

TABLE 1

Spot	DeCyder		Accession	Gene	Protein	Mascot		MW	pI	Matched	Cover.
Number	*Av Ratio Decid/crtl*	*p (t-test)*	*code*	*name*	*description*	*score*	*expect*	*/Da, theor.*	*theor.*	*peptides*	*%*
1	2,35	6,3E-04	gi|39777597	**TGM2**	**transglutaminase 2 isoform a**	228	1,4E-16	78420	5,11	6	13
2	1,97	4,6E-02	gi|119610097	P4HB	protein disulfide-isomerase	154	3,5E-09	21410	4,47	4	20
	1,97	4,6E-02	gi|15029922	RNH1	Ribonuclease inhibitor	154	3,5E-09	50104	4,83	4	12
3	-1,78	1,1E-02	gi|28723	**ACTN1**	**alpha-actinin**	137	1,8E-07	69061	5,07	8	15
4	3,37	1,1E-02	gi|741376	**CTSB**	**cathepsin B**	120	8,8E-06	17428	5,44	1	11
5	-1,99	4,9E-02	gi|67782365	KRT7	keratin 7	179	1,1E-11	51411	5,40	7	18
6	1,84	9,2E-04	gi|39777597	**TGM2**	**transglutaminase 2 isoform a**	111	7,0E-05	78420	5,11	4	8
7	1,82	1,6E-02	gi|5453790	NNMT	nicotinamide N-methyltransferase	159	1,1E-09	30011	5,56	4	17
8	2,08	1,9E-03	gi|4185720	UCHL1	ubiquitin carboxy-terminal hydrolase L1	183	4,4E-12	23354	5,30	4	25
	2,08	1,9E-03	gi|39777597	**TGM2**	**transglutaminase 2 isoform a**	148	1,4E-08	78420	5,11	6	9
	2,08	1,9E-03	gi|4185720	UCHL1	ubiquitin carboxy-terminal hydrolase L1	187	1,8E-12	23354	5,3	5	27
9	2,22	4,9E-02	gi|15277503	ACTB	beta actin	170	2,2E-12	40536	5,55	4	15
10	2,02	1,3E-02	gi|178045	ACTG1	gamma-actin	133	1,1E-08	26147	5,65	3	16
11	-1,88	3,8E-02	gi|188619	MMP3	matrix metalloproteinase-3	204	3,5E-14	54229	5,61	4	8
12	1,60	5,8E-03	gi|5453549	PRDX4	peroxiredoxin 4	187	1,8E-12	30749	5,86	5	24
13	-2,34	4,3E-02	gi|15149465	CALD1	caldesmon 1 isoform 5	225	7,0E-18	61233	6,40	9	23
14	-2,45	1,6E-02	gi|179830	CALD1	caldesmon	247	1,8E-18	62715	6,18	5	15
15	-1,56	4,1E-02	gi|3820535	TXNRD1	thioredoxin reductase GRIM-12	295	2,8E-23	55321	6,36	8	20
	-1,56	4,1E-02	gi|38044288	GSN	gelsolin isoform b	109	2,8E-06	80876	5,58	4	5
16	-1,82	3,1E-02	gi|4502101	ANXA1	annexin I	83	1,1E-03	38918	6,57	6	28
	-1,82	3,1E-02	gi|5453710	LASP1	LIM and SH3 protein 1	140	2,2E-09	30097	6,61	7	29
	-1,82	3,1E-02	gi|5668560	PPP1CC	serine/threonine phosphatase 1 gamma	83	1,1E-03	34493	5,09	6	16
17	2,01	6,1E-03	gi|67782309	SOD2	superoxide dismutase [Mn], mitochondrial	138	3,5E-09	20882	8,36	3	17
18	1,50	4,6E-02	gi|181969	EEF2	elongation factor 2	93	1,2E-04	40264	5,81	1	3
20	2,17	9,5E-03	gi|67782309	SOD2	superoxide dismutase [Mn], mitochondrial	260	2,2E-21	22290	6,86	6	34
21	2,04	6,8E-03	gi|32454741	SERPINH1	serpin H1	94	7,9E-05	46525	8,75	1	2
22	-1,55	2,0E-02	gi|55960374	TAGLN2	transgelin 2	235	2,8E-17	21244	7,63	8	42
23	-1,56	5,0E-02	gi|75516490	HNRPA1	heterogeneous nuclear ribonucleoprotein A1	144	8,9E-10	16806	9,71	3	27
24	1,70	2,3E-02	gi|226007	MYL1	ventricular myosin L1	91	1,9E-04	22123	4,97	1	6
25	1,78	3,0E-02	gi|39777597	**TGM2**	**transglutaminase 2 isoform a**	289	2,9E-24	78420	5,11	11	22
26	-1,52	3,6E-03	gi|5031877	LMNB1	lamin B1	100	2,5E-05	66653	5,11	3	7
27	1,75	2,1E-02	gi|62087548	LCP1	L-plastin variant	129	2,9E-08	56196	5,21	1	3
28	1,57	2,0E-02	gi|741376	**CTSB**	**cathepsin B**	192	1,4E-14	28595	5,23	7	25
29	-1,43	8,7E-03	gi|938026	RANBP1	Ran-binding protein 1	92	1,6E-04	23396	5,19	1	6
30	3,20	1,3E-02	gi|741376	**CTSB**	**cathepsin B**	137	2,1E-07	17428	5,44	1	11

31	1,76	4,0E-02	gi|741376	**CTSB**	**cathepsin B**	173	1,1E-12	28595	5,23	4	20
	1,76	4,0E-02	gi|119620391	CCTB	chaperonin containing TCP1, subunit 4 (CRA_b)	121	1,8E-07	28595	5,23	5	12
32	-1,45	4,3E-02	gi|4501891	ACTN1	actinin, alpha 1 isoform b	387	4,5E-34	1E+05	5,25	25	40
	-1,45	4,3E-02	gi|12025678	ACTN4	actinin, alpha 4	166	5,7E-12	1E+05	5,27	14	22
33	-1,40	2,9E-03	gi|1617118	PRDX2	Peroxiredoxin-2	139	2,9E-09	18486	5,19	3	21
34	1,89	3,2E-02	gi|662841	HSP27	heat shock protein 27	228	3,6E-18	22427	7,83	7	37
35	-1,51	1,6E-02	gi|5453990	PSME1	proteasome activator subunit 1 isoform 1	135	7,2E-09	28876	5,78	8	29
36	-1,42	2,3E-02	gi|35068	NME1	Nucleoside diphosphate kinase A	147	4,5E-10	20740	7,07	4	26
37	-1,81	4,5E-03	gi|116805340	GARS	glycyl-tRNA synthetase	139	2,9E-09	83854	6,61	4	5
38	1,85	4,3E-02	gi|662841	HSP27	heat shock protein 27	157	4,5E-11	22427	7,83	5	33
39	3,97	3,6E-02	gi|37181873	C1QTNF6	Complement C1q TNF-related protein 6	144	9,1E-10	29093	5,81	3	13
40	1,57	1,5E-02	gi|17389815	TPI1	Triosephosphate isomerase 1	179	2,9E-13	26910	6,45	5	28
41	2,22	2,2E-02	gi|21361176	ALDH1A1	aldehyde dehydrogenase 1A1	244	9,1E-20	55454	6,30	6	16
42	1,74	2,0E-02	gi|61656609	TRAP1	TNF receptor-associated protein 1	123	5,2E-06	57426	7,21	4	9
43	2,08	2,0E-02	gi|37747855	TF	transferrin	98	4,0E-05	79310	6,97	6	11
44	-2,48	2,5E-02	gi|48255905	**TAGLN**	**transgelin**	244	9,1E-20	22653	8,87	9	50
45	2,83	5,3E-04	gi|38202207	MAOB	monoamine oxidase B	170	2,3E-12	59238	7,20	7	16
46	-1,63	9,9E-03	gi|4758018	CNN2	calponin 2 isoform a	116	5,8E-07	34074	6,95	2	8
47	1,55	2,1E-02	gi|51242953	MGLL	monoglyceride lipase isoform 2	149	1,3E-08	33468	6,49	4	16
48	1,97	2,1E-02	gi|67782309	SOD2	superoxide dismutase 2, mitochondrial isoform B	178	1,6E-11	20882	8,36	5	30
49	1,47	2,4E-02	gi|55664661	VDAC2	voltage-dependent anion channel 2	220	2,3E-17	30842	8,00	6	26
50	1,55	2,7E-03	gi|115430223	LGALS3	galectin 3	258	3,6E-21	26193	8,57	9	35
51	1,40	1,8E-02	gi|595267	HADHA	Gastrin-binding protein	106	5,7E-06	83730	9,13	2	3
52	-2,22	4,3E-02	gi|48255905	**TAGLN**	**transgelin**	298	3,6E-25	22653	8,87	13	65
53	-1,42	2,4E-02	gi|4506631	RPL30	ribosomal protein L30	112	1,4E-06	12947	9,65	2	24

TABLE 2

Protein Name[a]	Fold Change[b]	p-value(%)[c]	Description[d]
MPIF-1	7,02	0.001	C-C motif chemokine 23
IGFBP-1	6,51	0.001	Insulin-like growth factor-binding protein 1
IL-10_R_beta	4,98	0.005	Interleukin-10 receptor subunit beta
IL-21R	4,49	0.0002	Interleukin-21 receptor
PECAM-1	4,20	0.0014	Platelet endotelial cell adhesión molecule 1
IL-1_R_II	3,39	0.001	Interleukin-1 receptor II
B7-1(CD80)	2,93	0.002	Activation B7-1 antigen
Leptin_R	2,74	0.001	Leptin receptor
IL-5_R_alpha	2,73	0.0001	Interleukin-5 receptor alpha
PRL	2,44	0.0004	Prolactin
IL-1_R4/ST2	2,39	0.002	Interleukin-1 receptor 4
IL-13_R_alpha_2	1,85	0.00	Interleukin-13 receptor alpha 2
Fas_Ligand	1,81	0.00	Tumor necrosis factor ligand superfamily member 6
L-Selectin	1,80	0.002	Leukocyte-endothelial cell adhesión molecule 1
IL-18_BP_alpha	1,64	0.00	Interleukin-18 bind protein alpha
ICAM-2	1,40	0.003	Intercellular adhesión molecule 2
IL-6	-2,31	0.00	Interleukin 6
MCP-3	-3,17	0.001	Chemokine ligand 7